

Multiparameter regularization and aggregation in the context of polynomial functional regression

Elke R. Gizewski^{a,b}, Markus Holzleitner^{c,*}, Lukas Mayer-Suess^d, Sergiy Pereverzyev Jr.^{a,b}, Sergei V. Pereverzyev^e

^aDepartment of Radiology, Medical University of Innsbruck Anichstrasse 35 6020, Innsbruck, Austria

^bNeuroimaging Research Core Facility, Medical University of Innsbruck Anichstrasse 35 6020, Innsbruck, Austria

^cMaLGA Center, Department of Mathematics, University of Genoa Via Dodecaneso 35 16146, Genoa, Italy

^dDepartment of Neurology, Medical University of Innsbruck Anichstrasse 35 6020, Innsbruck, Austria

^eJohann Radon Institute for Computational and Applied Mathematics, Austrian Academy of Sciences Altenberger Straße 69 A-4040, Linz, Austria

Abstract

Most of the recent results in polynomial functional regression have been focused on an in-depth exploration of single-parameter regularization schemes. In contrast, in this study we go beyond that framework by introducing an algorithm for multiple parameter regularization and presenting a theoretically grounded method for dealing with the associated parameters. This method facilitates the aggregation of models with varying regularization parameters. The efficacy of the proposed approach is assessed through evaluations on both synthetic and some real-world medical data, revealing promising results.

Keywords: Statistical learning theory, Functional polynomial regression, Multiparameter regularization, Aggregation
2020 MSC: Primary 65K10, Secondary 62G20

1. Introduction

Functional data analysis has emerged as a vibrant and dynamic research area and is present in various aspects of our daily lives, such as climate studies, medicine, economics, and healthcare, just to name a few. Typically, functional data appear in the forms of time series, shapes, images, and analogous objects. While the term "functional data analysis" was first used in [25, 26], significant advancements have happened since then. For a comprehensive exploration of methods, theory, and applications, we refer to seminal review articles like [16, 27, 28, 32], and also to the very recently appeared special issue [1].

This work focuses specifically on functional data inputs that are labeled with scalar-valued outputs. One of the most extensively studied methods in this context assumes a linear relationship between inputs and outputs, so that the outputs can be represented as linear functionals of the (functional) inputs, accompanied maybe by an additional noise term. One popular approach to capture linear functional regression is based on reproducing kernel Hilbert space (RKHS) techniques, so that the known arguments from kernel regression (see e.g. [6, 11, 17, 18]) can be used. A by no means complete list of works in this direction can be found in [30, 31, 34] and references therein. We may also mention [13], where linear functional regression approach is proposed in a more sophisticated setting of domain generalization.

Similarly to the case of extending standard linear regression by allowing polynomial interactions, polynomial functional regression (PFR), which includes the functional linear model and functional quadratic model as two special cases, was proposed in [22]. Then it has been discussed in [28, 29] and recently in [12], where a complete treatment of the interplay between smoothness, capacity and general one parameter regularization schemes is provided (as done

*Corresponding author

Email addresses: elke.gizewski@i-med.ac.at (Elke R. Gizewski), holzleitner@dima.unige.it (Markus Holzleitner), lukas.mayer@i-med.ac.at (Lukas Mayer-Suess), sergiy.pereverzyev@i-med.ac.at (Sergiy Pereverzyev Jr.), sergei.pereverzyev@oeaw.ac.at (Sergei V. Pereverzyev)

e.g. for standard kernel regression in [11, 18]). In particular, the study [12] has advocated the use of iterated one-parameter Tikhonov regularization method in the context of PFR.

One drawback of using single-parameter (iterated) Tikhonov regularization is, that all norms of the individual monomials in the regularization term are given equal weight, and therefore the advantage of using higher order monomials is not developed to its fullest potential. Consequently, it is advisable to introduce specific weight parameters for each individual monomial, and we envision it as a good place to advertise multi-parameter regularization in this context.

In general, multi-parameter (MP) regularization schemes have a rich history, both in terms of theory and applications, and we refer to [20][Chapter 3] and references therein for a comprehensive summary. It is interesting to note that the usage of multiple parameters has been judged variously by different authors. Just to give two examples: in [33], the authors found, that it provides only marginal improvements, whereas in [5] it is claimed that MP-regularization helps significantly, when the one parameter counterparts do not lead to satisfying results. One main finding of our work is, that in the case of PFR, we are in a similar situation as in [5], and one can demonstrate the advantage of using multi-parameter PFR in numerical examples based on synthetic toy data and on some real-world medical data.

At the same time, there is a common belief that the choice of the regularization parameters is crucial, and we are only aware of a few works that tackle this serious challenge in the MP case: a heuristic L-curve based strategy is proposed in [4], in [2, 3, 8] knowledge of the noise structure is required and in [19] an approach based on the discrepancy principle is discussed, which is costly to compute.

The solution that we will propose in the specific setting of PFR, is based on the so-called aggregation by the linear functional strategy, which may be traced back to [7] (see also Section 3.5 [24] and references therein). In the context of standard scalar and vector valued regression such type of aggregation has recently lead to successful performances in domain adaptation, a field that in many aspects is very sensitive to parameter selection as well, see e.g. [9, 10]. However, we are not aware of any works that employ the aggregation techniques in the context of functional data with MP regularization yet, and thus another main part of our study is to provide theoretical and numerical evidence, that aggregation can be successfully applied in these settings as well.

The main findings of this work can therefore be summarized as follows:

- We introduce multi-parameter regularization in the context of PFR and derive a linear system that allows us to compute the corresponding solutions.
- In order to deal with turning of multiple regularization parameters, we propose an aggregation procedure in the context of PFR.
- We provide numerical evidence, that MP regularization and aggregation can be useful concepts for PFR also in practice, on the one hand on synthetic data, and on the other hand, on data from a medical application, where the task is to detect stenosis in brain arteries.

Our work will now be structured as follows. In Section 2, we will recall the setting of regularized PFR, by repeating the definitions, assumptions and estimates from [12]. In Section 3, an algorithm how to compute the solution associated to MP-PFR is discussed, whereas Section 4 proposes an aggregation strategy for PFR, which can be evaluated numerically and which comes with additional theoretical guarantees. Section 5 is then devoted to the experiments on synthetic and real-world medical data.

2. Setting

2.1. Overall setting and assumptions

Let $\mathbb{I} \subset \mathbb{R}^d$ and consider the associated space $L^2(\mathbb{I})$ consisting of square integrable functions with respect to the Lebesgue measure μ , so that

$$\|u\|_{L^2(\mathbb{I})}^2 = \int_{\mathbb{I}} |u(t)|^2 d\mu(t).$$

Moreover, let $L^2(\Omega, \mathbb{P})$ be a space of random variables $Y = Y(\omega)$ defined on a probability space $(\Omega, \mathcal{F}, \mathbb{P})$, $\omega \in \Omega$, with bounded second moments, so that

$$\|Y\|_{L^2(\Omega, \mathbb{P})}^2 := \mathbb{E}|Y|^2 = \int_{\Omega} |Y(\omega)|^2 d\mathbb{P}(\omega).$$

Consider also the tensor product $L^2(\Omega, \mathbb{P}) \otimes L^2(\mathbb{I})$, which is nothing but a collection of random variables $X(\omega, s)$ indexed by points $s \in \mathbb{I}$ and having bounded second moments in the following sense:

$$\|X\|_{\mathbb{P}, \mu}^2 := \mathbb{E} \|X(\omega, \cdot)\|_{L^2(\mathbb{I})}^2.$$

The inner products in the considered Hilbert spaces \mathcal{H} will always be denoted by $\langle \cdot, \cdot \rangle_{\mathcal{H}}$, and the space is indicated by a subscript.

Functional data consist of random i.i.d. samples of functions $X_1(s), \dots, X_N(s)$, that can be seen as realizations of a stochastic process $X(\omega, s) \in L^2(\Omega, \mathbb{P}) \otimes L^2(\mathbb{I})$. Now let us discuss the setting of polynomial functional regression (PFR): Let $Y \in L^2(\Omega, \mathbb{P})$ be a scalar response, and $X \in L^2(\Omega, \mathbb{P}) \otimes L^2(\mathbb{I})$ be the corresponding functional predictor. We make the following assumption on X (as imposed in a similar way, e.g., in [31, 34]):

Assumption 1.

$$\sup_{\omega \in \Omega} \|X(\omega, \cdot)\|_{L^2(\mathbb{I})} \leq \kappa.$$

In PFR one aims at minimizing the expected prediction risk:

$$\mathcal{E}(U_p(X)) = \mathbb{E} (|Y(\omega) - U_p(X(\omega, \cdot))|^2) \rightarrow \min, \quad (1)$$

where $U_p(X(\omega, \cdot))$ is a polynomial regression of order p :

$$U_p(X(\omega, \cdot)) = u_0 + \sum_{l=1}^p \int_{\mathbb{I}^l} u_l(s_1, \dots, s_l) \prod_{j=1}^l X(\omega, s_j) d\mu(s_j).$$

Here $u_0 \in L^2_0 := \mathbb{R}$, and $u_l \in L^2_l$, where

$$L^2_l = \underbrace{L^2(\mathbb{I}) \otimes \dots \otimes L^2(\mathbb{I})}_{l\text{-times}}.$$

To proceed and formalize the setting further, consider the operator

$$A_0 : \mathbb{R} \rightarrow L^2(\Omega, \mathbb{P})$$

assigning to any $u_0 \in \mathbb{R}$ the corresponding constant random variable. Moreover, consider $A_l : L^2_l \rightarrow L^2(\Omega, \mathbb{P})$, such that

$$(A_l u)(\omega) = \int_{\mathbb{I}^l} u_l(s_1, \dots, s_l) \prod_{j=1}^l X(\omega, s_j) d\mu(s_j). \quad (2)$$

Let, also, $\mathbb{L}^2 = \bigoplus_{l=0}^p L^2_l$ be a direct sum of spaces L^2_l consisting of finite sequences $u = (u_0, \dots, u_p)$, $u_l \in L^2_l$, $l = 0, 1, \dots, p$, equipped with the norm $\|u\|_{\mathbb{L}^2}^2 = \sum_{l=0}^p \|u_l\|_{L^2_l}^2$, and consider the bounded linear operator (which is also a Hilbert-Schmidt one, as will be seen from Lemma 1) $\mathbb{A} : \mathbb{L}^2 \rightarrow L^2(\Omega, \mathbb{P})$, given by

$$\mathbb{A}u = (A_0, A_1, \dots, A_p) \circ (u_0, u_1, \dots, u_p) = \sum_{l=0}^p A_l u_l. \quad (3)$$

Observe that for any $u \in L^2(\Omega, \mathbb{P})$ the operator $A_l^* : L^2(\Omega, \mathbb{P}) \rightarrow L_l^2$ assigns to it the element

$$(A_l^*u)(s_1, \dots, s_l) = \int_{\Omega} u(\omega) \prod_{i=1}^l X(\omega, s_i) d\mathbb{P}(\omega),$$

and therefore, $\mathbb{A}^* \mathbb{A}$ is a $(p+1) \times (p+1)$ matrix of the operators

$$\mathbb{A}^* \mathbb{A} = \{A_k^* A_l : L_l^2 \rightarrow L_k^2, k, l = 0, 1, \dots, p\}$$

, where $A_0^* A_0 u_0 = u_0$ and

$$\begin{aligned} A_0^* A_l u &= \int_{\Omega} \int_{\mathbb{I}^l} u(s_1, \dots, s_l) \prod_{i=1}^l X(\omega, s_i) d\mu(s_i) d\mathbb{P}(\omega), \\ A_k^* A_l u(s_1, \dots, s_k) &= \int_{\Omega} \prod_{j=1}^k X(\omega, s_j) \int_{\mathbb{I}^l} u(\tilde{s}_1, \dots, \tilde{s}_l) \prod_{i=1}^l X(\omega, \tilde{s}_i) d\mu(\tilde{s}_i) d\mathbb{P}(\omega), \\ &k, l = 1, \dots, p. \end{aligned}$$

Equipped with this notation, we can write that $U_p(X(\omega, \cdot)) = \mathbb{A}u$, such that (1) is reduced to the least square solution of the equation $\mathbb{A}u = Y$, because $\mathcal{E}(U_p(X)) = \|Y - \mathbb{A}u\|_{L^2(\Omega, \mathbb{P})}^2$. Let us also use the following standard assumption:

Assumption 2. *The projection $\mathcal{P}Y$ of Y on the closure of the range of \mathbb{A} is such that $\mathcal{P}Y \in \text{Range}(\mathbb{A})$.*

It is well known (see, e.g., [20][Proposition 2.1.]), that under Assumption 2 the minimizer $u = u^+ = (u_0^+, \dots, u_p^+)$ of (1) solves the normal equation $\mathbb{A}^* \mathbb{A}u = \mathbb{A}^* Y$.

We will also use the fact that for any $u \in \mathbb{L}^2$

$$\|\mathbb{A}u\|_{L^2(\Omega, \mathbb{P})} = \left\| \sqrt{\mathbb{A}^* \mathbb{A}} u \right\|_{\mathbb{L}^2}, \quad (4)$$

which follows immediately from the polar decomposition of the operator \mathbb{A} .

For the further analysis let us also adopt the following response noise model:

Assumption 3.

$$Y = \mathbb{A}u^+ + \varepsilon, \quad (5)$$

where a noise variable $\varepsilon : \Omega \rightarrow \mathbb{R}$ is independent from X , $\mathbb{E}(\varepsilon) = 0$, and for some $\sigma > 0$ it should satisfy either the condition

$$\mathbb{E}(|\varepsilon(\omega)|^2) \leq \sigma^2, \quad (6)$$

or obey, for any integer $\tilde{m} \geq 2$ and some $M > 0$, a slightly stronger moment condition, which is also standard in the literature, see e.g. [30],

$$\mathbb{E}(|\varepsilon(\omega)|^{\tilde{m}}) \leq \frac{1}{2} \sigma^2 \tilde{m}! M^{\tilde{m}-2}. \quad (7)$$

However, the involved operators are inaccessible, because we do not know \mathbb{P} . Thus, we want to approximate them by using training data $(Y_i, X_i(\cdot))$, $i = 1, \dots, N$, consisting of N independent samples of the response and the functional predictor $(Y(\omega), X(\omega, \cdot))$, so that

$$Y_i = \mathbb{A}_i u^+ + \varepsilon_i,$$

where \mathbb{A}_i is defined in the same way as \mathbb{A} by the replacement of $X(\omega, \cdot)$ in the formulas (2) and (3) with $X_i(\cdot)$, and ε_i is a sample from the noise variable introduced in Assumption 3.

Moreover, u^+ does not depend continuously on the initial datum, such that we need to employ a regularization.

The simplest and arguably most well known regularization in this context is the single-parameter Tikhonov regularization, so for $\lambda > 0$ we want to find the minimizer u_λ of the regularized PFR

$$\|Y - \mathbb{A}u\|_{L^2(\Omega, \mathbb{P})}^2 + \lambda \|u\|_{\mathbb{L}^2}^2 \rightarrow \min, \quad (8)$$

which solves the equation $\lambda u + \mathbb{A}^* \mathbb{A} u = \mathbb{A}^* Y$ and can be approximated by the solution u_λ^N of

$$\lambda u + [\mathbb{A}^* \mathbb{A}]_N u = [\mathbb{A}^* Y]_N. \quad (9)$$

These approximations are given by $[\mathbb{A}^* \mathbb{A}]_N = \{[A_k^* A_l]_N : L_l^2 \rightarrow L_k^2, k, l = 0, 1, \dots, p\}$ so that:

$$\begin{aligned} [A_0^* A_0]_N u &= u, \\ [A_0^* A_l]_N u &= \frac{1}{N} \sum_{i=1}^N \int_{\mathbb{I}^l} u(s_1, \dots, s_l) \prod_{j=1}^l X_i(s_j) d\mu(s_j), \\ [A_k^* A_l]_N u(s_1, \dots, s_k) &= \frac{1}{N} \sum_{i=1}^N \prod_{j=1}^k X_i(s_j) \int_{\mathbb{I}^l} u(\tilde{s}_1, \dots, \tilde{s}_l) \prod_{m=1}^l X_i(\tilde{s}_m) d\mu(\tilde{s}_m), \\ &k, l = 1, \dots, p. \end{aligned} \quad (10)$$

and $[\mathbb{A}^* Y]_N = ([A_0^* Y]_N, \dots, [A_p^* Y]_N) \in \mathbb{L}^2$, so that

$$\begin{aligned} [A_0^* Y]_N &= \frac{1}{N} \sum_{i=1}^N Y_i, \\ [A_l^* Y]_N(s_1, \dots, s_l) &= \frac{1}{N} \sum_{i=1}^N Y_i \prod_{j=1}^l X_i(s_j), \\ &l = 1, \dots, p. \end{aligned} \quad (11)$$

A thorough analysis of one-parameter regularized PFR has been executed in [12] for a generalized regularization scheme, see e.g. Theorem 1 for their main finding.

Yet, when considering the single-parameter regularization within the realm of PFR, it could be contended that this might not be the most suitable selection. This approach overlooks individual contributions associated with monomials of varying degrees, treating them all with equal weight. In this context, a more fitting alternative for PFR is the employment of MP regularization, a choice that we will discuss thoroughly in Section 3. But before that let us move on by collecting several auxiliary results, which have mostly been derived already in [12].

2.2. Operator norms and related auxiliary estimates

Here we collect several estimates related to the norms of the previously discussed operators. Most of these results have been discussed in [12].

Lemma 1 (Lemma 1 in [12]). *Let $HS(\mathcal{H}_1, \mathcal{H}_2)$ denote the Hilbert space of Hilbert-Schmidt operators between Hilbert spaces \mathcal{H}_1 and \mathcal{H}_2 . For simplicity let us also use $HS(\mathcal{H}_1, \mathcal{H}_1) = HS(\mathcal{H}_1)$. Under Assumption 1 we have that*

$$\begin{aligned} \|\mathbb{A}\|_{HS(\mathbb{L}^2, L^2(\Omega, \mathbb{P}))} &\leq \tilde{\kappa} =: \sum_{l=0}^p k^l \\ \|\mathbb{A}^* \mathbb{A}\|_{HS(\mathbb{L}^2)}, \|[A^* \mathbb{A}]_N\|_{HS(\mathbb{L}^2)} &\leq \tilde{\kappa}^2 \end{aligned}$$

Lemma 2 (Lemma 2 in [12]). *For any $\delta \in (0, 1)$, with confidence at least $1 - \delta$ we have that*

$$\|\mathbb{A}^* \mathbb{A} - [A^* \mathbb{A}]_N\|_{\mathbb{L}^2 \rightarrow \mathbb{L}^2} \leq \|\mathbb{A}^* \mathbb{A} - [A^* \mathbb{A}]_N\|_{HS(\mathbb{L}^2)} \leq \frac{4\tilde{\kappa}^2}{\sqrt{N}} \log \frac{2}{\delta} \quad (12)$$

Lemma 3 (compare with Lemma 4 in [12]). *For any $\delta \in (0, 1)$, with confidence at least $1 - \delta$ we have that in case of noise assumption (6):*

$$\|[\mathbb{A}^* \mathbb{A}]_N u^+ - [\mathbb{A}^* Y]_N\|_{\mathbb{L}^2} \leq \frac{\sigma \tilde{\kappa}}{\sqrt{N} \delta}, \quad (13)$$

whereas in case of (7):

$$\|[\mathbb{A}^* \mathbb{A}]_N u^+ - [\mathbb{A}^* Y]_N\|_{\mathbb{L}^2} \leq \frac{(M + \sigma) \tilde{\kappa} \log(2/\delta)}{\sqrt{N}}. \quad (14)$$

Lemma 3 can, to some extent, be seen as a special case of Lemma 4 in [12], however, in order to introduce notation and techniques required for some further technical results as e.g. Lemma 6, we still decided to provide its proof here:

To this end we also need to recall the following well-known concentration bound:

Lemma 4 (see e.g. Theorem 3.3.4. in [35]). *Let ξ be a random variable with values in a Hilbert space \mathcal{H} . Let $\{\xi_1, \xi_2, \dots, \xi_N\}$ be a sample of N independent observations of ξ . Furthermore, assume that the bound $\mathbb{E}\|\xi\|_{\mathcal{H}}^{\tilde{m}} \leq \frac{\nu}{2} \tilde{m}! u^{\tilde{m}-2}$ holds for every $2 \leq \tilde{m} \in \mathbb{N}$, then for any $0 < \delta < 1$ with confidence at least $1 - \delta$ we have*

$$\left\| \frac{1}{N} \sum_{i=1}^N [\xi_i - \mathbb{E}(\xi)] \right\|_{\mathcal{H}} \leq \frac{2u \log(2/\delta)}{N} + \sqrt{\frac{2\nu \log(2/\delta)}{N}}$$

Proof of Lemma 3. Let us first focus on the more involved estimate (14). The estimate (13) can be proven by similar reasoning. Consider the matrix of operators

$$\mathcal{A}(\omega) = \{ \mathcal{A}_{k,l}(\omega) : L_l^2 \rightarrow L_l^2(\Omega, \mathbb{P}) \otimes L_k^2, k, l = 0, \dots, p \},$$

where $\mathcal{A}_{0,0}u(\omega) = u$, $\mathcal{A}_{0,l}u(\omega) = (A_l u)(\omega)$,

$$\mathcal{A}_{k,l}u(\omega, s_1, \dots, s_k) = \prod_{j=1}^k X(\omega, s_j) \int_{\mathbb{I}^l} u(\tilde{s}_1, \dots, \tilde{s}_l) \prod_{m=1}^l X(\omega, \tilde{s}_m) d\tilde{s}_m \quad (15)$$

$$k, l = 1, \dots, p, \omega \in \Omega.$$

Then the operators \mathcal{A}^i , $i = 1, \dots, N$, defined by using $X_i(\cdot)$ instead of $X(\omega, \cdot)$ in the above formulas, can be seen as independent observations of $\mathcal{A}(\omega)$.

It is clear that $\mathbb{E}(\mathcal{A}(\omega)) = \mathbb{A}^* \mathbb{A}$ and that $\|\mathcal{A}(\omega)\|_{\text{HS}(\mathbb{L}^2)} \leq \tilde{\kappa}^2$, so that $\mathcal{A}(\omega)$ is a random variable in $\text{HS}(\mathbb{L}^2)$. Moreover we introduce the vectors $\mathcal{X}(\omega) \in L^2(\Omega, \mathbb{P}) \otimes \mathbb{L}^2$,

$$\mathcal{X}(\omega) = (\mathcal{X}_k(\omega))_{k=0}^p, \quad \mathcal{X}_0(\omega) = 1, \quad \mathcal{X}_k(\omega) = \prod_{j=1}^k X(\omega, s_j), \quad k = 1, \dots, p, \quad (16)$$

with $\|\mathcal{X}(\omega)\|_{\mathbb{L}^2} \leq \tilde{\kappa}$, and the \mathbb{L}^2 -valued random variable

$$\xi(\omega) = (Y(\omega) - \mathbb{A}(\omega)u^+) \mathcal{X}(\omega) = \varepsilon(\omega) \mathcal{X}(\omega),$$

where the last equality is due to Assumption 3. Then the functions

$$\xi_i = Y_i \mathcal{X}^i - \mathcal{A}^i u^+,$$

where \mathcal{X}^i are defined by using $X_i(\cdot)$ instead of $X(\omega, \cdot)$ in (16), can be seen as independent observations of $\xi(\omega)$. Moreover we have:

$$\frac{1}{N} \sum_{i=1}^N \xi_i = \frac{1}{N} \sum_{i=1}^N Y_i \mathcal{X}^i - \frac{1}{N} \sum_{i=1}^N \mathcal{A}^i u^+,$$

so that for $k = 0, \dots, p$, recalling (11):

$$\left(\frac{1}{N} \sum_{i=1}^N Y_i \mathcal{X}^i \right)_k (s_1, \dots, s_k) = \frac{1}{N} \sum_{i=1}^N Y_i \prod_{j=1}^k X_i(s_j) = [A_k^* Y]_N (s_1, \dots, s_k), \quad (17)$$

and recalling (10):

$$\left(\frac{1}{N} \sum_{i=1}^N \mathcal{A}^i u^+ \right)_k (s_1, \dots, s_k) = \frac{1}{N} \sum_{i=1}^N \sum_{l=0}^p \prod_{j=1}^k X_i(s_j) \int_{\mathbb{I}^l} u_l^+(\tilde{s}_1, \dots, \tilde{s}_l) \prod_{m=1}^l X_i(\tilde{s}_m) d\mu(\tilde{s}_m) = ([\mathbb{A}^* \mathbb{A}]_N u^+)_k (s_1, \dots, s_k), \quad (18)$$

which allows us to conclude:

$$\frac{1}{N} \sum_{i=1}^N \xi_i = [\mathbb{A}^* Y]_N - [\mathbb{A}^* \mathbb{A}]_N u^+.$$

Due to Assumption 3 we have

$$\mathbb{E}(\xi(\omega)) = \mathbb{E}(\mathcal{X}(\omega)) \mathbb{E}(\varepsilon(\omega)) = 0.$$

Moreover, the independence of ε and \mathcal{X} leads to the conclusion that:

$$\mathbb{E}(\|\xi\|_{\mathbb{I}^2}^{\tilde{m}}) \leq \mathbb{E}(\|\mathcal{X}(\omega)\|_{\mathbb{I}^2}^{\tilde{m}}) \cdot \mathbb{E}(|\varepsilon(\omega)|^{\tilde{m}}) \leq \frac{\sigma^2 \tilde{\kappa}^2}{2} (M\tilde{\kappa})^{\tilde{m}-2} \tilde{m}!.$$

Now the application of Lemma 4 for $\xi(\omega)$ and ξ_i yields the desired bound (14).

To obtain (13) we need to follow the same lines of proof, but only consider the case $\tilde{m} = 2$ and afterward apply Tschebyshev's inequality instead. □

3. Multiparameter regularization

Equipped with the necessary background and notation on PFR, let us continue our discussion on MP regularization in this context. Instead of dealing with (8) and using only a single parameter λ , we consider a vector $\lambda = (\lambda_0, \dots, \lambda_p)$ of the regularization parameters $\lambda_l \geq 0$, $l = 0, \dots, p$, and the corresponding regularization functional with multiple penalties:

$$\|Y - \mathbb{A}u\|_{L^2(\Omega, \mathbb{P})}^2 + \sum_{l=0}^p \lambda_l \|u_l\|_{L^2}^2 \rightarrow \min. \quad (19)$$

Next, let $P_l : \mathbb{I}^2 \rightarrow \mathbb{I}^2$, $l = 0, \dots, p$, be the projection of \mathbb{I}^2 onto L_l^2 , i.e. $P_l(u_0, \dots, u_p) = (0, \dots, 0, u_l, 0, \dots, 0)$, so that clearly $\|P_l u\|_{\mathbb{I}^2} = \|u_l\|_{L_l^2}$. Then (19) can equivalently be written as

$$\|Y - \mathbb{A}u\|_{L^2(\Omega, \mathbb{P})}^2 + \sum_{l=0}^p \lambda_l \|P_l u\|_{\mathbb{I}^2}^2 \rightarrow \min,$$

and using arguments similar to those given in [20, Formula (3.12)], we can easily make the following observation:

Lemma 5. *The minimizer u_λ of (19) solves the equation*

$$\sum_{l=0}^p \lambda_l P_l u + \mathbb{A}^* \mathbb{A} u = \mathbb{A}^* Y. \quad (20)$$

Proof. The Frechét derivative of $F(u) = \|Y - \mathbb{A}u\|_{L^2(\Omega, \mathbb{P})}^2$ in direction $v \in \mathbb{L}^2$ is given by $F'(u)(v) = \langle 2(\mathbb{A}^* \mathbb{A}u - \mathbb{A}^* Y), v \rangle_{\mathbb{L}^2}$, and that of $F_l(u) = \lambda_l \|P_l u\|_{\mathbb{L}^2}^2$ by $F'_l(u)(v) = 2\lambda_l \langle P_l^* P_l u, v \rangle_{\mathbb{L}^2} = 2\lambda_l \langle P_l u, v \rangle_{\mathbb{L}^2}$. Setting the derivative of $F + \sum_{l=0}^p F_l$ to zero and using the convexity of the problem under consideration we arrive at (20). \square

Next we employ a Monte-Carlo type discretization of (20) and approximate the minimizer of (19) by the solution u_λ^N of

$$\sum_{l=0}^p \lambda_l P_l u + [\mathbb{A}^* \mathbb{A}]_N u = [\mathbb{A}^* Y]_N \quad (21)$$

In view of (10), (11) the regularized approximation u_λ^N can be constructed in the form $u_\lambda^N = (u_{\lambda,0}^N, u_{\lambda,1}^N, \dots, u_{\lambda,p}^N) \in \mathbb{L}^2$, so that

$$\begin{aligned} u_{\lambda,0}^N &= b_0 \in \mathbb{R}, \\ u_{\lambda,l}^N(s_1, \dots, s_l) &= \sum_{i=1}^N b_{l,i} \prod_{j=1}^l X_i(s_j) \in L_l^2, \quad l = 1, \dots, p. \end{aligned}$$

Inserting this ansatz into (21) and equating the corresponding coefficients we obtain the following system of $pN+1$ linear equations for b_0 and $b_{k,i}$, $k = 1, \dots, p$, $i = 1, \dots, N$:

$$(\lambda_0 + 1)b_0 + \frac{1}{N} \sum_{i=1}^N \sum_{l=1}^p \sum_{s=1}^N b_{l,s}(c_{i,s})^l = \frac{1}{N} \sum_{i=1}^N Y_i, \quad (22)$$

$$\lambda_k b_{k,i} + \frac{1}{N} b_0 + \frac{1}{N} \sum_{l=1}^p \sum_{s=1}^N b_{l,s}(c_{i,s})^l = \frac{1}{N} Y_i, \quad (23)$$

where $c_{i,s} = \int_{\mathbb{H}} X_i(\tilde{s}) X_s(\tilde{s}) d\mu(\tilde{s})$. Note that for single-parameter regularization, i.e. for the case of $\lambda = \lambda_0 = \dots = \lambda_p$, the system (22), (23) allows for a reduction to a linear system of only $N+1$ equations. This was discussed in detail in Section 3 of [12].

A crucial issue, however, is the choice of the regularization parameters $\lambda_0, \dots, \lambda_p$. In Section 1 we already mentioned several approaches to this issue. But most of them select just one set of parameters. On the other hand, it seems more practical to use all values from a grid of parameters and then aggregate all the resulting models, such that even badly chosen regularization parameters can in the end contribute to an improved model. In the next section we will theoretically justify an aggregation method in the context of PFR and also observe its usefulness in the empirical evaluations in Sections 5.1–5.2.

4. Aggregation of multiple regularized polynomial functional models

To continue with a discussion of an aggregation strategy in the PFR context, let us now assume that we are given a sequence of models $u_1, \dots, u_R \in \mathbb{L}^2$, so that the following assumption is valid:

Assumption 4.

$$\|u^+\|_{\mathbb{L}^2}, \|u_r\|_{\mathbb{L}^2} \leq C_R$$

for $r = 1, \dots, R$ and some $C_R > 0$.

Our goal is to compute an aggregation

$$\sum_{r=1}^R c_r u_r \quad (24)$$

with coefficients $c_1, \dots, c_R \in \mathbb{R}$, so that the excess of risk $\mathcal{E}(\sum_{r=1}^R c_r u_r) - \mathcal{E}(u^+)$ is as small as possible. We already know from (4) and (5) that

$$\mathcal{E}(u) - \mathcal{E}(u^+) = \|\mathbb{A}(u - u^+)\|_{L^2(\Omega, \mathbb{P})}^2 = \left\| \sqrt{\mathbb{A}^* \mathbb{A}}(u - u^+) \right\|_{\mathbb{L}^2}^2, \quad (25)$$

for any $u \in \mathbb{L}^2$, so that our main objective can be written as follows:

$$\min_{c_1, \dots, c_R \in \mathbb{R}} \left\| \sqrt{\mathbb{A}^* \mathbb{A}} \left(\sum_{r=1}^R c_r u_r - u^+ \right) \right\|_{\mathbb{L}^2}^2. \quad (26)$$

Next we observe that the minimizer of (26), i.e. the best approximation u^* of the target regression function u^+ by linear combinations, corresponds to the vector $c^* = (c_1^*, \dots, c_R^*)$ of ideal coefficients in (24) that solves the linear system $Gc^* = \bar{g}$ with the Gram matrix

$$G = \left(\left\langle \sqrt{\mathbb{A}^* \mathbb{A}} u_r, \sqrt{\mathbb{A}^* \mathbb{A}} u_{r'} \right\rangle_{\mathbb{L}^2} \right)_{r, r'=1}^R = \left(\langle \mathbb{A} u_r, \mathbb{A} u_{r'} \rangle_{L^2(\Omega, \mathbb{P})} \right)_{r, r'=1}^R$$

and the vector

$$\bar{g} = \left(\left\langle \sqrt{\mathbb{A}^* \mathbb{A}} u^+, \sqrt{\mathbb{A}^* \mathbb{A}} u_r \right\rangle_{\mathbb{L}^2} \right)_{r=1}^R = \left(\langle \mathbb{A} u^+, \mathbb{A} u_r \rangle_{L^2(\Omega, \mathbb{P})} \right)_{r=1}^R$$

(see e.g. [24, Section 3.5.] for a proof of this well known observation).

Note that the successful inversion of G depends on the assumption that our models exhibit sufficient dissimilarity. This requirement is inherent, as without it, we could effortlessly eliminate redundant models. But, of course, neither Gram matrix G nor the vector \bar{g} is accessible, because there is no access to \mathbb{P} , so we switch to the empirical counterparts \tilde{G} and \tilde{g} , i.e.

$$\tilde{G} = \left(\frac{1}{N} \sum_{i=1}^N (\mathbb{A}_i u_r)(\mathbb{A}_i u_{r'}) \right)_{r, r'=1}^R \quad (27)$$

$$\tilde{g} = \left(\frac{1}{N} \sum_{i=1}^N Y_i (\mathbb{A}_i u_r) \right)_{r=1}^R. \quad (28)$$

Then we compute the solution $\tilde{c} = (\tilde{c}_1, \dots, \tilde{c}_R)$ to the system $\tilde{G}\tilde{c} = \tilde{g}$, so that our aggregated model is given by

$$\tilde{u} = \sum_{r=1}^R \tilde{c}_r u_r. \quad (29)$$

Our main result is about the quality of this aggregation computed from data, and we show that $\mathcal{E}(\tilde{u}) - \mathcal{E}(u^+)$ approaches $2(\mathcal{E}(u^*) - \mathcal{E}(u^+))$ when the sample size increases:

Theorem 1. *Under assumptions 1 – 4 with probability $1 - \delta$ it holds that for sufficiently large N*

$$\mathcal{E}(\tilde{u}) - \mathcal{E}(u^+) \leq 2(\mathcal{E}(u^*) - \mathcal{E}(u^+)) + CN^{-1} \log^2 \frac{1}{\delta}, \quad (30)$$

where the coefficient $C > 0$ does not depend on N and δ .

According to our theorem, the excess of risk of the proposed algorithm is asymptotically not worse than twice the excess of risk of the unknown optimal aggregation, because it is clear (see, e.g., Corollary 1 in [12]) that the second term in the right hand side of (30) is negligibly small.

The proof of this result will crucially depend on the following Lemma, which relates the entries of G and \tilde{G} and \bar{g} and \tilde{g} , respectively:

Lemma 6. *Under assumptions 1 – 4 with probability $1 - \delta$ we have that for any $r, r' = 1, \dots, R$:*

$$\left| \langle \mathbb{A}u_r, \mathbb{A}u_{r'} \rangle_{L^2(\Omega)} - \frac{1}{N} \sum_{i=1}^N \mathbb{A}_i u_r \mathbb{A}_i u_{r'} \right| \leq \frac{C \log \frac{2}{\delta}}{\sqrt{N}}, \quad (31)$$

$$\left| \langle \mathbb{A}u^+, \mathbb{A}u_r \rangle_{L^2(\Omega)} - \frac{1}{N} \sum_{i=1}^N Y_i \mathbb{A}_i u_r \right| \leq \frac{C \log \frac{2}{\delta}}{\sqrt{N}}, \quad (32)$$

where C is some generic constant C , which does not depend on N or δ .

Proof. Let us start by showing (31). Observe that in view of (10) we have

$$\frac{1}{N} \sum_{i=1}^N \mathbb{A}_i u_r \mathbb{A}_i u_{r'} = \frac{1}{N} \sum_{i=1}^N \langle \mathcal{X}_i, u_r \rangle_{\mathbb{L}^2} \langle \mathcal{X}_i, u_{r'} \rangle_{\mathbb{L}^2} = \langle [\mathbb{A}^* \mathbb{A}]_N u_r, u_{r'} \rangle_{\mathbb{L}^2},$$

Then

$$\langle \mathbb{A}^* \mathbb{A} u_r, u_{r'} \rangle_{\mathbb{L}^2} = \langle [\mathbb{A}^* \mathbb{A}]_N u_r, u_{r'} \rangle_{\mathbb{L}^2} + \langle (\mathbb{A}^* \mathbb{A} - [\mathbb{A}^* \mathbb{A}]_N) u_r, u_{r'} \rangle_{\mathbb{L}^2},$$

and it remains to estimate the last term to arrive at (31):

$$|\langle (\mathbb{A}^* \mathbb{A} - [\mathbb{A}^* \mathbb{A}]_N) u_r, u_{r'} \rangle_{\mathbb{L}^2}| \leq \| \mathbb{A}^* \mathbb{A} - [\mathbb{A}^* \mathbb{A}]_N \|_{\mathbb{L}^2 \rightarrow \mathbb{L}^2} \|u_r\|_{\mathbb{L}^2} \|u_{r'}\|_{\mathbb{L}^2} \leq C_R^2 \frac{4\tilde{\kappa}^2}{\sqrt{N}} \log \frac{2}{\delta},$$

where we used Cauchy-Schwartz inequality, Lemma 2 and Assumption 4.

Now let us deal with (32). It is clear from (17) that

$$\langle [\mathbb{A}^* Y]_N, u_r \rangle_{\mathbb{L}^2} = \frac{1}{N} \sum_{i=1}^N Y_i \langle \mathcal{X}_i, u_r \rangle_{\mathbb{L}^2} = \frac{1}{N} \sum_{i=1}^N Y_i \mathbb{A}_i u_r.$$

Then we can continue as follows:

$$\langle \mathbb{A}^* \mathbb{A} u^+, u_r \rangle_{\mathbb{L}^2} = \langle [\mathbb{A}^* Y]_N, u_r \rangle_{\mathbb{L}^2} + \underbrace{\langle (\mathbb{A}^* \mathbb{A} - [\mathbb{A}^* \mathbb{A}]_N) u^+, u_r \rangle_{\mathbb{L}^2}}_{(I)} + \underbrace{\langle [\mathbb{A}^* \mathbb{A}]_N u^+ - [\mathbb{A}^* Y]_N, u_r \rangle_{\mathbb{L}^2}}_{(II)}.$$

For (I) we apply Lemma 2, Assumption 4 and Cauchy-Schwartz inequality to obtain the bound:

$$(I) \leq C_R^2 \frac{4\tilde{\kappa}^2}{\sqrt{N}} \log \frac{2}{\delta},$$

whereas for (II) we use (13) or (14) and again Assumption 4 and Cauchy-Schwartz to have:

$$(II) \leq C_R^2 \frac{C}{\sqrt{N}} \log \frac{2}{\delta},$$

where the constant C may be different, depending on whether noise assumption (6) or (7) is in force. Now (32) follows by combining (I) and (II). \square

Now we can use similar arguments as used, e.g., in the proof of Theorem 1 of [9]. In the sequel, $\|\cdot\|_{\mathbb{R}^R}$ and $\|\cdot\|_{\mathbb{R}^R \rightarrow \mathbb{R}^R}$ denote the usual Euclidean and the Frobenius norm, respectively. From Lemma 6 we can argue that with probability $1 - \delta$ it holds:

$$\|\bar{g} - \tilde{g}\|_{\mathbb{R}^R} \leq C \log \frac{1}{\delta} N^{-\frac{1}{2}}, \quad (33)$$

$$\|G - \tilde{G}\|_{\mathbb{R}^R \rightarrow \mathbb{R}^R} \leq C \log \frac{1}{\delta} N^{-\frac{1}{2}}. \quad (34)$$

It is also straightforward to bound the entries of \tilde{G} uniformly:

$$|\tilde{G}_{r,r'}| \leq \|[\mathbb{A}^* \mathbb{A}]_N\|_{\mathbb{L}^2 \rightarrow \mathbb{L}^2} \|u_r\|_{\mathbb{L}^2} \|u_{r'}\|_{\mathbb{L}^2} \leq \tilde{\kappa}^2 C_R^2.$$

Moreover we can use the following simple manipulation:

$$G^{-1} = \tilde{G}^{-1}(G\tilde{G}^{-1})^{-1} = \tilde{G}^{-1}(I - (I - G\tilde{G}^{-1}))^{-1} = \tilde{G}^{-1}(I - (\tilde{G} - G)\tilde{G}^{-1})^{-1}.$$

Then using the Neumann series for $(I - (\tilde{G} - G)\tilde{G}^{-1})^{-1}$ we obtain the following bound:

$$\|G^{-1}\|_{\mathbb{R}^R \rightarrow \mathbb{R}^R} \leq \frac{\|\tilde{G}^{-1}\|_{\mathbb{R}^R \rightarrow \mathbb{R}^R}}{1 - \|\tilde{G}^{-1}\|_{\mathbb{R}^R \rightarrow \mathbb{R}^R} \|G - \tilde{G}\|_{\mathbb{R}^R \rightarrow \mathbb{R}^R}} \leq c. \quad (35)$$

To see (35), we first observe that it is natural to assume that $\|\tilde{G}^{-1}\| \leq c$ for some generic $c > 0$ (otherwise, we can, e.g., orthogonalize our models and coefficients without changing the aggregation, but with reducing the condition number $\|\tilde{G}^{-1}\| \|\tilde{G}\|$). Secondly, by (34) it is also natural to assume that $\|G - \tilde{G}\|_{\mathbb{R}^R \rightarrow \mathbb{R}^R} < \frac{1}{2c}$ by choosing N sufficiently large. Therefore the Neumann series associated to $(I - (\tilde{G} - G)\tilde{G}^{-1})^{-1}$ converges, since $\|(\tilde{G} - G)\tilde{G}^{-1}\|_{\mathbb{R}^R \rightarrow \mathbb{R}^R} < \frac{1}{2}$. This allows to deduce $\|G^{-1}\|_{\mathbb{R}^R \rightarrow \mathbb{R}^R} \leq 2c$. Now we are in the position to prove our main generalization bound (30):

Proof of Theorem 1. Since:

$$G^{-1}(\tilde{g} - \bar{g}) + G^{-1}(G - \tilde{G})\tilde{c} = G^{-1}\tilde{g} - c^* + \tilde{c} - G^{-1}\tilde{g} = \tilde{c} - c^*,$$

we can use (33)–(35) and Hölder's inequality to claim that for sufficiently large N with probability $1 - \delta$ it holds

$$\|\tilde{c} - c^*\|_{\mathbb{R}^R}^2 \leq 2 \|G^{-1}\|_{\mathbb{R}^R \rightarrow \mathbb{R}^R}^2 \left(\|\tilde{g} - \bar{g}\|_{\mathbb{R}^R}^2 + \|G - \tilde{G}\|_{\mathbb{R}^R \rightarrow \mathbb{R}^R}^2 \|\tilde{c}\|_{\mathbb{R}^R}^2 \right) \leq CN^{-1} \log^2 \frac{1}{\delta} \quad (36)$$

Moreover:

$$\begin{aligned} \mathcal{E}(\tilde{u}) - \mathcal{E}(u^+) &= \left\| \sqrt{\mathbb{A}^* \mathbb{A}}(\tilde{u} - u^+) \right\|_{\mathbb{L}^2}^2 \\ &\leq \left(\left\| \sqrt{\mathbb{A}^* \mathbb{A}}(u^* - u^+) \right\|_{\mathbb{L}^2} + \left\| \sqrt{\mathbb{A}^* \mathbb{A}}(\tilde{u} - u^*) \right\|_{\mathbb{L}^2} \right)^2 \\ &\leq 2 \left\| \sqrt{\mathbb{A}^* \mathbb{A}}(u^* - u^+) \right\|_{\mathbb{L}^2}^2 + 2 \left\| \sqrt{\mathbb{A}^* \mathbb{A}}(\tilde{u} - u^*) \right\|_{\mathbb{L}^2}^2 \\ &= 2(\mathcal{E}(u^*) - \mathcal{E}(u^+)) + 2 \left\| \sqrt{\mathbb{A}^* \mathbb{A}}(\tilde{u} - u^*) \right\|_{\mathbb{L}^2}^2 \\ &\leq 2(\mathcal{E}(u^*) - \mathcal{E}(u^+)) + 2 \left(\sum_{r=1}^R |c_r^* - \tilde{c}_r| \left\| \sqrt{\mathbb{A}^* \mathbb{A}} u_r \right\|_{\mathbb{L}^2} \right)^2 \\ &\leq 2(\mathcal{E}(u^*) - \mathcal{E}(u^+)) + 2R \|c^* - \tilde{c}\|_{\mathbb{R}^R}^2 \max_r \left\| \sqrt{\mathbb{A}^* \mathbb{A}} u_r \right\|_{\mathbb{L}^2}^2 \\ &\leq 2(\mathcal{E}(u^*) - \mathcal{E}(u^+)) + 2R \left\| \sqrt{\mathbb{A}^* \mathbb{A}} \right\|_{\mathbb{L}^2 \rightarrow \mathbb{L}^2}^2 C_R^2 \|c^* - \tilde{c}\|_{\mathbb{R}^R}^2, \end{aligned} \quad (37)$$

The statement of the theorem follows now from (36)–(37). \square

5. Experimental evaluation

5.1. Toy example

In this section we use a toy example to demonstrate the advantage of MP regularization and aggregation. To this end, as an explanatory variable, we consider a random process

$$X(\omega, t) = \sum_{k=0}^5 \xi_k(\omega) \cos(kt), t \in [0, 2\pi],$$

where $\xi_k(\omega)$ are random variables uniformly distributed on $[-1, 1]$. Consider also the response variable $Y(\omega)$ related to the explanatory variable $X(\omega, t)$ as follows:

$$Y(\omega) = u_0^+ + \int_0^{2\pi} X(\omega, t) u_1^+(t) d\mu(t) + \int_0^{2\pi} \int_0^{2\pi} X(\omega, t) X(\omega, \tau) u_2^+(t, \tau) d\mu(t) d\mu(\tau).$$

In our simulations, we use $u^+ = (u_0^+, u_1^+, u_2^+)$ with

$$u_0^+ = 2, u_1^+ = 1 + 4 \cos t + \cos 5t, u_2^+ = \cos 3t + \cos 2t \cos 2\tau.$$

We simulate N independent samples $(Y_i, X_i(\cdot))$ of $(Y(\omega), X(\omega, t))$ and use them to construct the regularized quadratic approximation $u_\lambda^N = (u_{\lambda,0}^N, u_{\lambda,1}^N, u_{\lambda,2}^N)$ of $u^+ = (u_0^+, u_1^+, u_2^+)$ by MP regularization as described in Section 3, for 27 different values of λ , so that all possible choices of $\lambda_0, \lambda_1, \lambda_2 \in \{10^{-5}, 10^{-7}, 10^{-9}\}$ are considered.

On Figure 1 we plot the error $\|u^+ - u_\lambda^N\|_{\mathbb{L}^2}$ against the number of the used samples $N = 1, 2, \dots, 40$, for these 27 choices of λ . In several cases (e.g. $\lambda_0 = \lambda_1 = 10^{-9}, \lambda_2 = 10^{-7}$) it is clearly visible that choosing different values of $\lambda_0, \lambda_1, \lambda_2$ can be advantageous compared to the case of one-parameter regularization $\lambda_0 = \lambda_1 = \lambda_2$. We also observe that the error curves corresponding to all the computed models saturate at low values (roughly ~ 3.14) for $N \geq 27$.

Next, to see the advantage of combining all the 27 computed models in terms of an aggregation as discussed in Section 4, in Figure 2 we even observe saturation at ~ 3.14 already at $N \geq 21$. Let us also mention, that we provided an implementation in Pytorch [23]. This allows the code to leverage GPU acceleration, enabling fast computation of the involved integrals.

These results look promising, therefore in order to underpin the usefulness of our method, we show experiments on real world medical data in the next subsection.

5.2. Stenosis Data

In this section, we demonstrate an application of MP-PFR and the associated aggregation approach presented in Sections 3, 4 to the problem of automatic stenosis detection from lumen diameters. Stenosis refers to an abnormal narrowing of a blood vessel due to a lesion, leading to a reduction in the lumen's space. This pathology is particularly critical in cervical arteries, including internal carotid arteries (ICA) and vertebral arteries (VA), where stenosis can impede or block blood flow to the brain, significantly elevating the risk of a stroke. Consequently, the automatic detection of stenosis becomes a crucial challenge in neuroradiology.

This detection issue typically arises in the final or quantification stage of computerized tomography (CT) or magnetic resonance imaging (MRI) angiography, when the vessel lumen segmentation and centerline extraction have already been executed. The detection mentioned above is the result of all work in the earlier stages, and therefore deserves special attention. Following the segmentation of CT/MRI scans, the existing software facilitates the estimation of vessel cross-section diameters, denoted as d_s ($s = 1, 2, \dots$, approximately 500), at various positions t_s along the vessel centerlines. Given the variability in positions t_s and their total numbers across different patients, it is natural to organize these data in the form of functions $X(t)$. For instance, cubic interpolation splines with knots at t_s can describe the diameter variation, with the values $X(t_s)$ corresponding to d_s ($s = 1, 2, \dots$). This approach allows clinical data to be represented as a samples (X_i, Y_i) consisting of functional inputs $X_i = X_i(t)$ ($i = 1, 2, \dots, N$) labeled by outputs Y_i which are assigned the value of 0 for a diagnosis indicating no stenosis, and values of 0.25, 0.5, 0.75, 1.0 for diagnoses

representing light, medium, moderate, or high stenosis, respectively. With the use of this dataset, a predictor can be constructed to automatically detect the presence or absence of stenosis by assigning an appropriate label Y to the corresponding profile $X(t)$ of variations in vessel cross-section diameters.

We have permission for research-driven secondary use of anonymized clinical data collected at the Department of Radiology and Department of Neurology, Medical University of Innsbruck, within the ReSect-study [21]. In our experiments below, we use the data about $N = 40$ ICA. The available data sample contains only 7 arteries affected by stenosis, and we need to ensure their inclusion in both the training and test sets. To achieve this, we opt for a random train-test split, so that the training set will consistently comprise of data of 16 ICA without stenosis and 4 ICA with stenosis, while the test set will consist of data of 17 non-stenosis arteries and 3 stenosis-affected ones.

Recall that in the present context, the variables $X(t)$ are functions of the position t along vessel centerlines, and the lengths of that centerlines vary from patient to patient. Therefore, in order to compute the integrals required in the algorithms of Sections 3 and 4, we confine the inputs to a specific interval $\mathbb{I} = [0, b]$, where b is the minimum length observed in the available clinical data. In our experiments, we use $b = 140$ mm. Moreover, let us also mention that similar to Section 5.1, also here we use Pytorch [23] for our implementations, so that the code is GPU-compatible and allows for fast computation of the involved integrals.

We construct the models u_λ as described in (22)–(23), for both linear and quadratic functional regression, and for all possible choices of $\lambda_0, \lambda_1, \lambda_2 \in \{10^{-2}, 10^{-1}, 1\}$. Afterward, we compute an aggregation \tilde{u} of all u_λ corresponding to the different choices of λ , again both for linear and quadratic case. Hereby we use the approach from Section 4, i.e. we solve the system associated to (27)–(28) and then combine the aggregation function (29). For a given functional data sample X_i , the predicted value is then computed as $f(X_i) = \mathbb{A}_i u_\lambda$, or $f(X_i) = \mathbb{A}_i \tilde{u}$, respectively. Note also that when a continuous-valued predictor $f(X_j)$ is used as binary classifier, its diagnostic ability depends on the so-called discrimination threshold c , such that a particular artery corresponding to an input X_i is assumed to be affected by stenosis if $f(X_i) > c$. In our experiments, we choose $c = 0.5$.

It is known that in medical statistics the accuracy of prediction of the presence or absence of a medical condition is mathematically described in terms of sensitivity (SE) and specificity (SP). Recall that SE is calculated as $\frac{TP}{TP+FN}$, while $SP = \frac{TN}{TN+FP}$. Here, TP represents the instances where a stenosis in the examined artery is identified by both the reference standard and the algorithm, irrespective of its severity (given the preventive measures for even mild narrowing of the cervical artery). TN accounts for cases where no stenosis in the considered artery is detected by both the reference standard and the algorithm. Meanwhile, FN and FP denote the respective counts of cases where the algorithm incorrectly identifies the absence or presence of stenosis.

The diagnostic efficacy of a specific classifier can also be effectively evaluated using the receiver/relative operating characteristic (ROC) curve. This graphical representation illustrates the diagnostic performance of f across varying discrimination thresholds. The ROC curve is constructed by plotting the sensitivity (SE) against the complement of specificity ($1 - SP$) for different threshold settings.

The outcomes of ROC analysis can be succinctly summarized using a single metric, namely the area under the ROC curve (AUC). The AUC ranges from approximately 0.5 for randomly assigned diagnoses to 1.0, indicating perfect diagnostic classification. In the subsequent analysis, we present the performance of the considered classifiers based on test inputs, considering all the aforementioned metrics and assuming that all classifiers use the same threshold $c = 0.5$.

Our results for the linear and quadratic case are depicted in Tables 1 and 2. We report the performance measure as an average over 10 runs, both linear, quadratic and aggregated models use the same data for training and testing in each run, so that a fair comparison is provided.

We can make the following important observations:

1. MP regularisation leads to better results than the single parameter counterpart both for linear and quadratic functional regression.
2. Aggregation is a reliable strategy to address the issue of dealing with multiple regularisation parameters and, especially in the quadratic case, significantly improves performance.
3. In the context of stenosis detection, SE is more important than SP, because it is less dangerous to misdetect a pathology than to misdetect its absence. From this viewpoint, in the present study the aggregation demonstrates an ability to stabilize performance of linear functional regression. Moreover, the results reported in Tables 1

Parameters	SE	SP	AUC
$\lambda_0 = 1, \lambda_1 = 1$	0.333333	0.988235	0.915686
$\lambda_0 = 1, \lambda_1 = 0.1$	0.4	0.952941	0.833333
$\lambda_0 = 1, \lambda_1 = 0.01$	0.333333	0.911765	0.668627
$\lambda_0 = 0.1, \lambda_1 = 1$	0.333333	1	0.915686
$\lambda_0 = 0.1, \lambda_1 = 0.1$	0.4	0.958824	0.833333
$\lambda_0 = 0.1, \lambda_1 = 0.01$	0.333333	0.911765	0.668627
$\lambda_0 = 0.01, \lambda_1 = 1$	0.266667	1	0.933333
$\lambda_0 = 0.01, \lambda_1 = 0.1$	0.366667	0.964706	0.839216
$\lambda_0 = 0.01, \lambda_1 = 0.01$	0.333333	0.923529	0.67451
Aggregation	0.6	0.488235	0.641176

Table 1: Performance metrics for linear MP-FR, averaged over 10 runs.

and 2 for the aggregation clearly indicate that in terms of SE the quadratic approach outperforms its linear counterpart, that should not be always expected or taken for granted (see, e.g., [14]).

Let us conclude this section by comparing our results with some alternative approaches. The comprehensive survey [15] offers a thorough examination of algorithms designed for detecting stenosis based on vessel cross-section diameters, utilizing the same inputs as our considered methods. While the algorithms discussed in [15] were initially developed for coronary artery stenosis detection, they have the potential applicability to diagnose stenoses in various artery types, including ICA.

It seems that our algorithms demonstrates superior results compared to those reported in [15] (where the stated values were $SE = 0.55$ and $SP = 0.33$). At the same time, we would like to note that the application of polynomial functional regression to the problem of automatic stenosis detection from lumen diameters has been presented here for illustration purposes, and one may expect that nonlinear and non-polynomial functional regression methods may exhibit even better performance.

6. Acknowledgements

The research reported in this paper has been supported by the Federal Ministry for Climate Action, Environment, Energy, Mobility, Innovation and Technology (BMK), the Federal Ministry for Digital and Economic Affairs (BMDW), and the Province of Upper Austria in the frame of the COMET–Competence Centers for Excellent Technologies Programme and the COMET Module S3AI managed by the Austrian Research Promotion Agency FFG.

The data used in Section 5.2 was acquired through the ReSect-study performed at the Medical University of Innsbruck. This study is funded by the OeNB Anniversary Fund (15644).

This work is additionally co-funded by the European Union (ERC, SAMPDE, 101041040). Views and opinions expressed are however those of the authors only and do not necessarily reflect those of the European Union or the European Research Council. Neither the European Union nor the granting authority can be held responsible for them.

References

- [1] Germán Aneiros, Ivana Horová, Marie Hušková, and Philippe Vieu. On functional data analysis and related topics. *Journal of Multivariate Analysis*, 189:104861, 2022.
- [2] Frank Bauer and Sergei Pereverzev. An utilization of a rough approximation of a noise covariance within the framework of multi-parameter regularization. *Int. J. Tomogr. Stat.*, 4:1–12, 2006.
- [3] Frank Bauer, Sergei Pereverzyev, and Lorenzo Rosasco. On regularization algorithms in learning theory. *Journal of complexity*, 23(1):52–72, 2007.
- [4] Murat Belge, Misha E Kilmer, and Eric L Miller. Efficient determination of multiple regularization parameters in a generalized l-curve framework. *Inverse problems*, 18(4):1161, 2002.
- [5] Mikhail Belkin, Partha Niyogi, and Vikas Sindhwani. Manifold regularization: A geometric framework for learning from labeled and unlabeled examples. *Journal of machine learning research*, 7(11), 2006.
- [6] Andrea Caponnetto and Ernesto De Vito. Optimal rates for the regularized least-squares algorithm. *Foundations of Computational Mathematics*, 7(3):331–368, 2007.

Parameters	SE	SP	AUC
$\lambda_0 = 1, \lambda_1 = 1, \lambda_2 = 1$	0.6	0.482353	0.54902
$\lambda_0 = 1, \lambda_1 = 1, \lambda_2 = 0.1$	0.6	0.488235	0.552941
$\lambda_0 = 1, \lambda_1 = 1, \lambda_2 = 0.01$	0.6	0.488235	0.552941
$\lambda_0 = 1, \lambda_1 = 0.1, \lambda_2 = 1$	0.633333	0.417647	0.492157
$\lambda_0 = 1, \lambda_1 = 0.1, \lambda_2 = 0.1$	0.6	0.482353	0.54902
$\lambda_0 = 1, \lambda_1 = 0.1, \lambda_2 = 0.01$	0.6	0.488235	0.552941
$\lambda_0 = 1, \lambda_1 = 0.01, \lambda_2 = 1$	0.766667	0.270588	0.4
$\lambda_0 = 1, \lambda_1 = 0.01, \lambda_2 = 0.1$	0.633333	0.411765	0.490196
$\lambda_0 = 1, \lambda_1 = 0.01, \lambda_2 = 0.01$	0.6	0.482353	0.54902
$\lambda_0 = 0.1, \lambda_1 = 1, \lambda_2 = 1$	0.6	0.482353	0.54902
$\lambda_0 = 0.1, \lambda_1 = 1, \lambda_2 = 0.1$	0.6	0.488235	0.552941
$\lambda_0 = 0.1, \lambda_1 = 1, \lambda_2 = 0.01$	0.6	0.488235	0.552941
$\lambda_0 = 0.1, \lambda_1 = 0.1, \lambda_2 = 1$	0.633333	0.417647	0.492157
$\lambda_0 = 0.1, \lambda_1 = 0.1, \lambda_2 = 0.1$	0.6	0.482353	0.54902
$\lambda_0 = 0.1, \lambda_1 = 0.1, \lambda_2 = 0.01$	0.6	0.488235	0.552941
$\lambda_0 = 0.1, \lambda_1 = 0.01, \lambda_2 = 1$	0.766667	0.270588	0.4
$\lambda_0 = 0.1, \lambda_1 = 0.01, \lambda_2 = 0.1$	0.633333	0.411765	0.490196
$\lambda_0 = 0.1, \lambda_1 = 0.01, \lambda_2 = 0.01$	0.6	0.482353	0.54902
$\lambda_0 = 0.01, \lambda_1 = 1, \lambda_2 = 1$	0.6	0.482353	0.54902
$\lambda_0 = 0.01, \lambda_1 = 1, \lambda_2 = 0.1$	0.6	0.488235	0.552941
$\lambda_0 = 0.01, \lambda_1 = 1, \lambda_2 = 0.01$	0.6	0.488235	0.552941
$\lambda_0 = 0.01, \lambda_1 = 0.1, \lambda_2 = 1$	0.633333	0.417647	0.492157
$\lambda_0 = 0.01, \lambda_1 = 0.1, \lambda_2 = 0.1$	0.6	0.482353	0.54902
$\lambda_0 = 0.01, \lambda_1 = 0.1, \lambda_2 = 0.01$	0.6	0.488235	0.552941
$\lambda_0 = 0.01, \lambda_1 = 0.01, \lambda_2 = 1$	0.766667	0.270588	0.4
$\lambda_0 = 0.01, \lambda_1 = 0.01, \lambda_2 = 0.1$	0.633333	0.411765	0.490196
$\lambda_0 = 0.01, \lambda_1 = 0.01, \lambda_2 = 0.01$	0.6	0.482353	0.54902
Aggregation	0.8	0.441176	0.756863

Table 2: Performance metrics for quadratic MP-FR, averaged over 10 runs.

- [7] Jieyang Chen, Sergiy Pereverzyev Jr, and Yuesheng Xu. Aggregation of regularized solutions from multiple observation models. *Inverse Problems*, 31(7):075005, 2015.
- [8] Zhongying Chen, Yao Lu, Yuesheng Xu, and Hongqi Yang. Multi-parameter tikhonov regularization for linear ill-posed operator equations. *Journal of computational mathematics*, pages 37–55, 2008.
- [9] Marius-Constantin Dinu, Markus Holzleitner, Maximilian Beck, Hoan Duc Nguyen, Andrea Huber, Hamid Eghbal-Zadeh, Bernhard Moser, Sergei Pereverzyev, Sepp Hochreiter, and Werner Zellinger. Addressing parameter choice issues in unsupervised domain adaptation by aggregation. In *11 th International Conference on Learning Representations*, 2023.
- [10] Elke R Gizewski, Lukas Mayer, Bernhard A Moser, Duc Hoan Nguyen, Sergiy Pereverzyev Jr, Sergei V Pereverzyev, Natalia Shepeleva, and Werner Zellinger. On a regularization of unsupervised domain adaptation in rkhs. *Applied and Computational Harmonic Analysis*, 57:201–227, 2022.
- [11] Zheng-Chu Guo, Shao-Bo Lin, and Ding-Xuan Zhou. Learning theory of distributed spectral algorithms. *Inverse Problems*, 33(7):074009, 2017.
- [12] Markus Holzleitner and Sergei V Pereverzyev. On regularized polynomial functional regression. *to appear in Journal of Complexity*, 2024.
- [13] Markus Holzleitner, Sergei V Pereverzyev, and Werner Zellinger. Domain generalization by functional regression. *to appear in Numerical Functional Analysis and Optimization*, 2024.
- [14] Lajos Horváth and Ron Reeder. A test of significance in functional quadratic regression. *Bernoulli Society for Mathematical Statistics and Probability*, 19(5A):2120–2151, 2013.
- [15] HA Kirişli, Michiel Schaap, CT Metz, AS Dharampal, Willem Bob Meijboom, Stella-Lida Papadopoulou, Admir Dedic, Koen Nieman, Michiel A de Graaf, MFL Meijs, et al. Standardized evaluation framework for evaluating coronary artery stenosis detection, stenosis quantification and lumen segmentation algorithms in computed tomography angiography. *Medical image analysis*, 17(8):859–876, 2013.
- [16] Piotr Kokoszka and Matthew Reimherr. *Introduction to functional data analysis*. CRC press, 2017.
- [17] Shao-Bo Lin, Xin Guo, and Ding-Xuan Zhou. Distributed learning with regularized least squares. *The Journal of Machine Learning Research*, 18(1):3202–3232, 2017.

- [18] Shuai Lu, Peter Mathé, and Sergei V Pereverzev. Balancing principle in supervised learning for a general regularization scheme. *Applied and Computational Harmonic Analysis*, 48(1):123–148, 2020.
- [19] Shuai Lu and Sergei V Pereverzev. Multi-parameter regularization and its numerical realization. *Numerische Mathematik*, 118:1–31, 2011.
- [20] Shuai Lu and Sergei V Pereverzev. *Regularization theory for ill-posed problems: selected topics*, volume 58. Walter de Gruyter, 2013.
- [21] Lukas Mayer, Christian Boehme, Thomas Toell, Benjamin Dejakum, Johann Willeit, Christoph Schmidauer, Klaus Berek, Christian Siedentopf, Elke Ruth Gizewski, Gudrun Ratzinger, et al. Local signs and symptoms in spontaneous cervical artery dissection: a single centre cohort study. *Journal of Stroke*, 21(1):112, 2019.
- [22] Hans-Georg Müller and Fang Yao. Additive modelling of functional gradients. *Biometrika*, 97(4):791–805, 2010.
- [23] A. Paszke, S. Gross, F. Massa, A. Lerer, J. Bradbury, G. Chanan, T. Killeen, Z. Lin, N. Gimselshein, L. Antiga, et al. Pytorch: An imperative style, high-performance deep learning library. *arXiv preprint arXiv:1912.01703*, 2019.
- [24] Sergei Pereverzev. *An Introduction to Artificial Intelligence Based on Reproducing Kernel Hilbert Spaces*. Springer Nature, 2022.
- [25] James O Ramsay. When the data are functions. *Psychometrika*, 47:379–396, 1982.
- [26] James O Ramsay and C. J. Dalzell. Some tools for functional data analysis. *Journal of the Royal Statistical Society Series B: Statistical Methodology*, 53(3):539–561, 1991.
- [27] James O Ramsay and Bernard W Silverman. *Applied functional data analysis: methods and case studies*. Springer, 2002.
- [28] Philip T Reiss, Jeff Goldsmith, Han Lin Shang, and R Todd Ogden. Methods for scalar-on-function regression. *International Statistical Review*, 85(2):228–249, 2017.
- [29] Zhang Tao, Zhang Qingzhao, and Wang Qihua. Model detection for functional polynomial regression. *Computational Statistics and Data Analysis*, 70(4):83–197, 2014.
- [30] Hongzhi Tong. Distributed least squares prediction for functional linear regression. *Inverse Problems*, 38(2):025002, 2021.
- [31] Hongzhi Tong and Michael Ng. Analysis of regularized least squares for functional linear regression model. *Journal of Complexity*, 49:85–94, 2018.
- [32] Jane-Ling Wang, Jeng-Min Chiou, and Hans-Georg Müller. Functional data analysis. *Annual Review of Statistics and its application*, 3:257–295, 2016.
- [33] Peiliang Xu, Yoichi Fukuda, and Yumei Liu. Multiple parameter regularization: numerical solutions and applications to the determination of geopotential from precise satellite orbits. *Journal of Geodesy*, 80:17–27, 2006.
- [34] Ming Yuan and T Tony Cai. A reproducing kernel hilbert space approach to functional linear regression. *Annals of Statistics*, 6(38):3412 – 3444, 2010.
- [35] Vadim Yurinsky. *Sums and Gaussian Vectors*. Lecture Notes in Mathematics. Springer Berlin, Heidelberg, 1995.

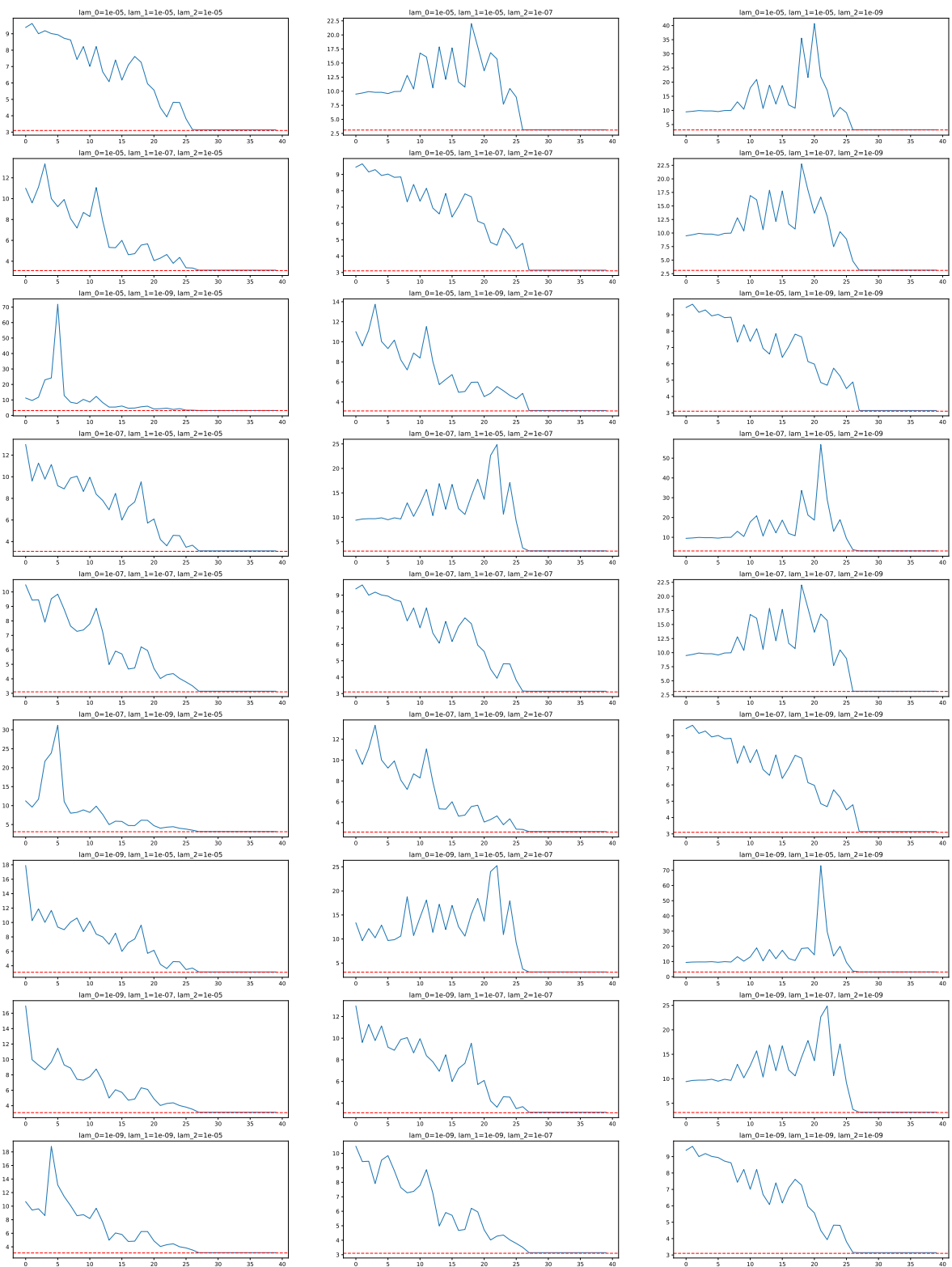


Figure 1: Error curves for all possible choices of λ . Red line depicts error rate of 3.14

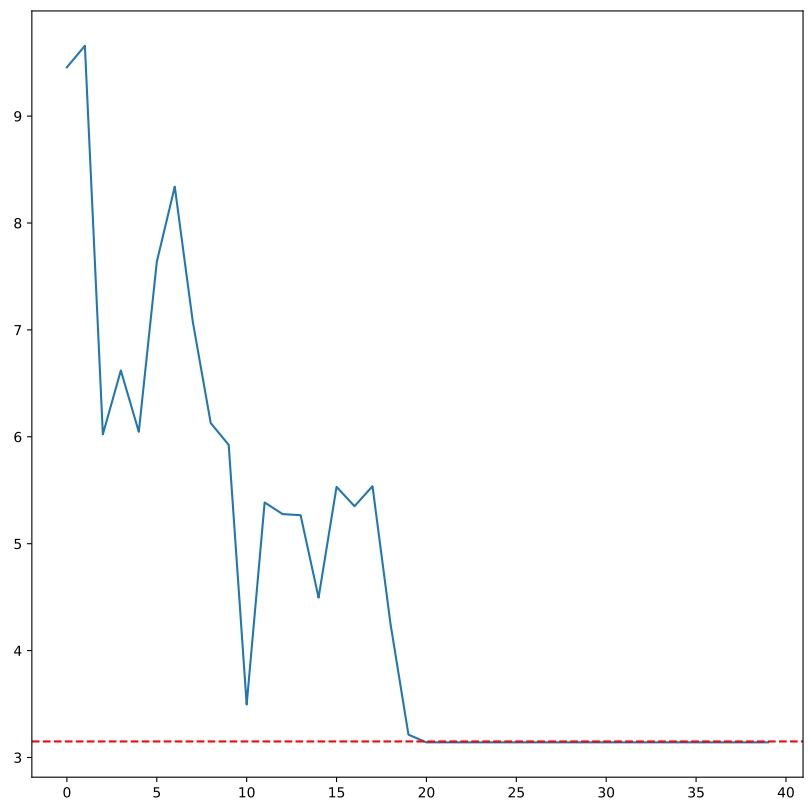


Figure 2: Error curve for aggregation. Red line depicts error rate of 3.14